

Supplemental Material: Model for screened, charge-regulated electrostatics of an eye lens protein: bovine gammaB-crystallin

I. DESCRIPTION OF SUPPLEMENTAL FIGURES AND TABLES

Figure 1: The quilted pattern in Fig. 1(a) shows the contribution of each pairing of the top-ranked 100 configurations at pH 7.1. The configuration probabilities are laid out as the lengths of line segments, in rank order from left to right and bottom to top, all within a square having side lengths 1. Therefore, the area of each rectangle gives the product of the probabilities of two of the top-ranked 100 patterns, an approximation to the probability of the occurrence of a given pair, ignoring biasing for simplicity. For example, the sum of the areas of the two rectangles outlined in yellow gives the probability that one member of a neighboring pair of proteins will be in configuration 1, while the other will be in configuration 7. The corresponding surface voltage maps of configurations 1 and 7 are shown in Figs. 1(b) and (c), respectively. Clearly, the study of numerous *pairs* of protonation configurations is needed to fill up the square in Fig. 1(a), to quantitatively model the relevant interactions.

Figure 2: Each of the prominent red bars in the perspective view of the work-of-charging shown in Fig. 2 has a magnitude $3 < 3\phi/k_B T < 8$ and corresponds to a charge pair or a charge triple involving either Glu or Asp residues and neighboring Lys or Arg residues.

Figure 3(a) illustrates Eq.(14) of the text, which im-

plies that for all protonation patterns sharing the same number of bound, titratable protons, plots of the logarithm of the pattern probability vs. pH will be congruent and vertically displaced from one another.

Figure 3(b) displays the joint dependence of pattern probabilities P_n on both pH and net charge, in which arches of $\log_{10} P_n$ vs. pH , like those in Fig. 3(a), link pattern probability points $(\log_{10} P_n, q_{net})$ in graphs of the $(\log_{10} P_n$ vs. protein net charge q_{net}). $(\log_{10} P_n, q_{net})$ graphs are shown for pH values of 7.1, 5.5, and 4.5, and are the same as those that appear in Fig. 12 of the text.

Figure 4 displays a table giving the number of times each residue switched protonation states during Monte Carlo simulations of 10^8 iterations, at a range of pH values.

Figure 5 displays a table giving the pK_{eff, α_*} values at pH 4.5 and 7.1 for each residue, together with those for which $pK_{1/2}$ was calculated. $pK_{1/2}$ values given in the table are those that occurred within the pH ranges of the sets of simulations used for generating Fig. 15(a) of the text. The remaining residues did not have $pK_{1/2}$ values within the selected range.

Figs. (6 and 7), (8 and 9), and (10 and 11) tabulate the work-of-charging matrices calculated for Debye screening lengths of 6Å, 12Å, and 20Å, respectively. Table entries are in the dimensionless units of $e\phi_{ij}/k_B T$. In each matrix, the order of residues is the same as that in Fig. 2 of the Supplementary Material, and in Figs. 3(a), 16(a), and 16(b) of the text.

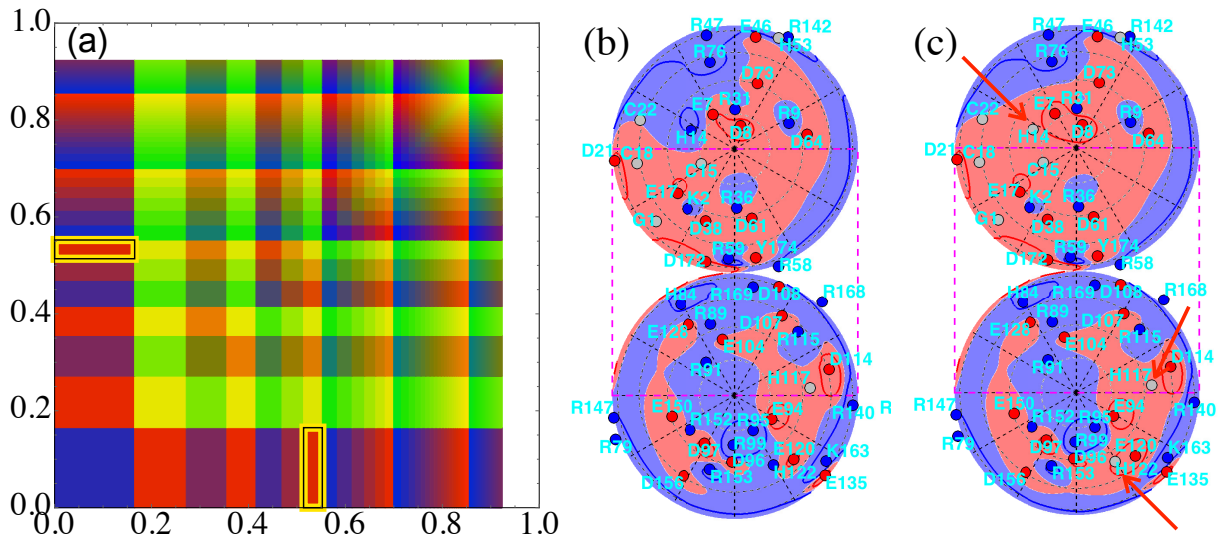


FIG. 1. (color online) (a) Illustration of the scope of the problem of estimating protein-protein interaction strengths while accounting for the probability distribution of protonation patterns, at pH 7.1 and Debye length 6 Å. Modeled configuration probabilities for isolated proteins are given by the lengths of line segments, proceeding in rank order from left to right and bottom to top, inside a square of area 1. The area of each rectangle approximates a configuration-pair probability (see text). (b) and (c): Surface voltage projections of configurations 1, in panel (b) and 7, in panel (c), whose joint probability is estimated by the area of the rectangles highlighted in yellow in (a).

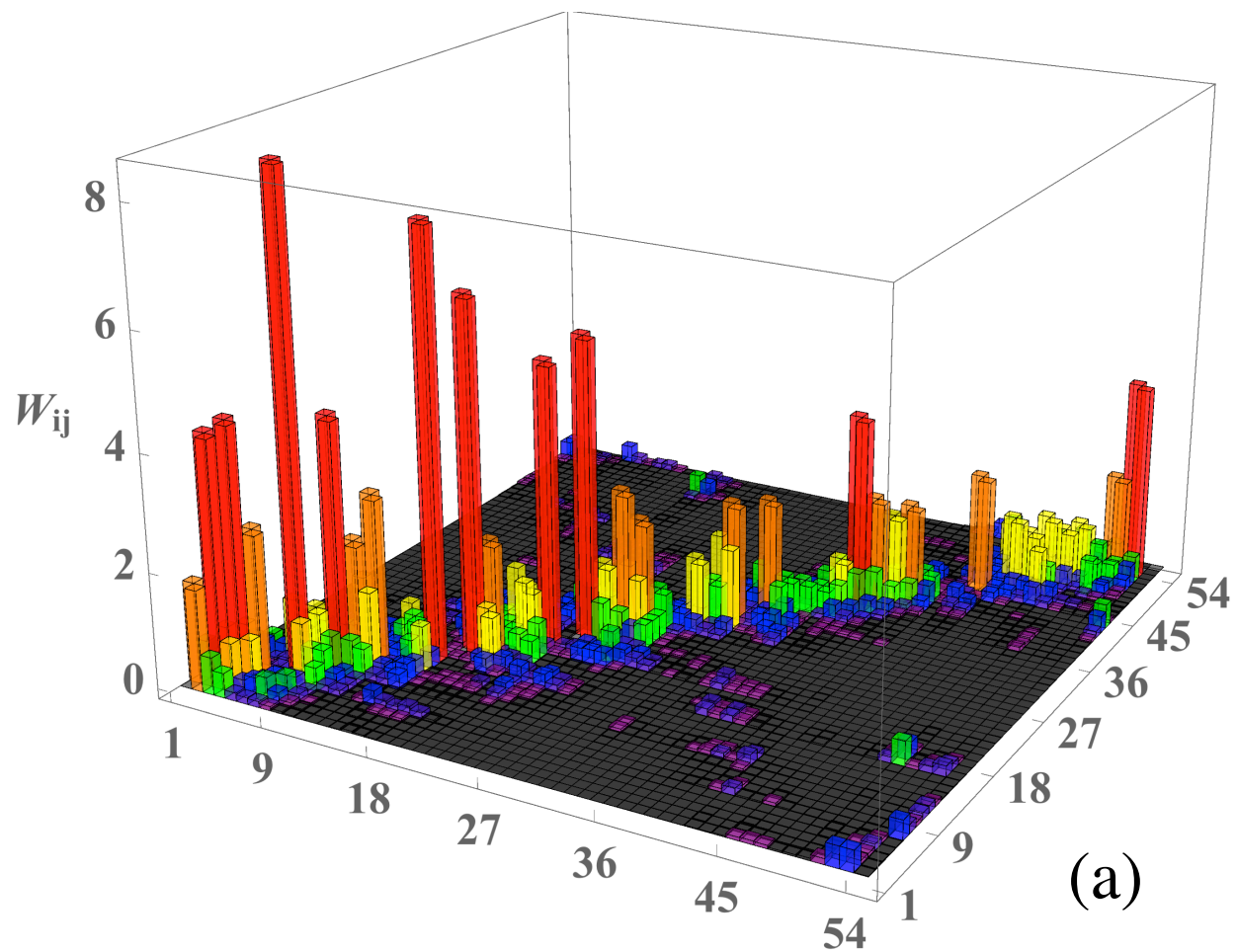


FIG. 2. (color online) (a): Perspective view of the work-of-charging entries W_{ij} used in the present model and displayed as a color map in Fig. 3(a) of the text. The vertical scale is in the units $e\phi/k_B T$, and the residue order and color code are also as in Fig. 3(a) of the text.

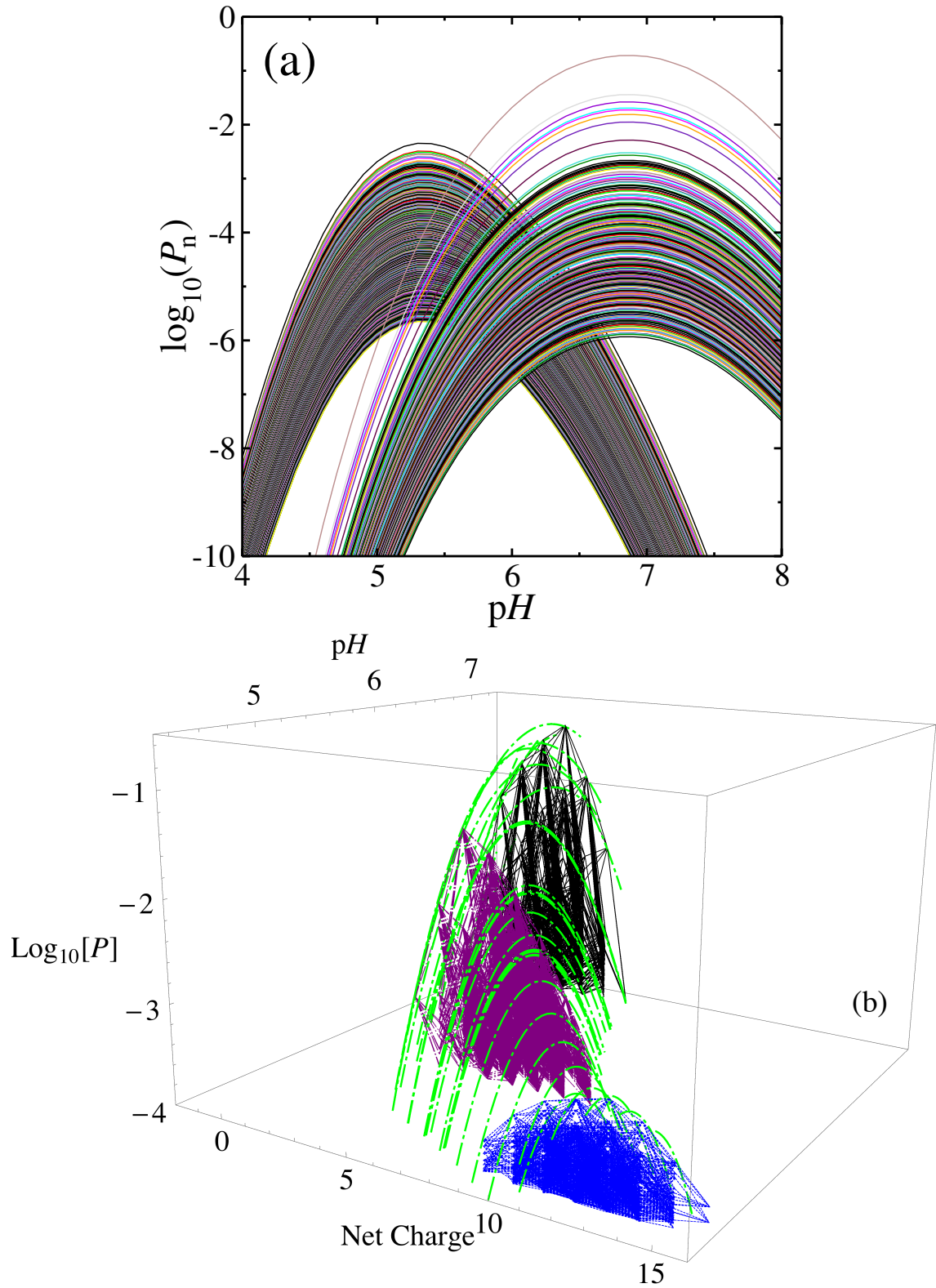


FIG. 3. (color online) (a) $\log_{10} P_\alpha$ vs. pH for protonation configurations α that have fixed titratable proton occupancies, n , of $n = 34$ (net charge $+8e$, arches with peaks near $\text{pH} = 5.3$) and $n = 28$ (net charge $+2e$, arches with peaks near $\text{pH} = 6.8$). The plot includes all such patterns that occurred in the Monte Carlo simulations at least once per million time steps. For configurations α having the same n , the congruence of the arches illustrates Eq. (14) in the text. (b) Illustration of the combined dependence of configuration probabilities on pH and net protein charge; the fixed pH patterns in Fig. 12 of the text are shown (black, solid - $\text{pH} 7.1$; blue, dash-dotted - $\text{pH} 5.5$; purple, dotted - $\text{pH} 4.5$) together with topmost pH dependence configuration probability arches like those in Fig. 14(a) of the text (green, dash-dotted).

Index	Residue	pK _{eff}	pH								
			4.0	4.5	5.0	5.5	6.0	6.5	7.0	7.5	8.0
1	ARG009	12.45	0	2	0	2	0	8	22	40	94
2	ARG031	12.90	0	0	0	0	0	2	6	14	38
3	ARG036	14.04	0	2	0	0	0	0	0	4	8
4	ARG047	11.33	4	2	6	4	30	84	172	580	1768
5	ARG058	10.70	4	6	6	10	60	204	700	2154	6514
6	ARG059	14.66	0	0	0	0	0	0	0	0	0
7	ARG076	11.50	0	0	2	6	10	30	104	350	1072
8	ARG079	9.48	76	158	248	614	1522	4320	12284	34827	99532
9	ARG089	14.33	0	0	0	0	0	0	0	0	0
10	ARG091	11.88	0	0	4	0	2	30	40	144	420
11	ARG095	11.54	0	0	0	6	14	32	102	276	802
12	ARG099	11.47	0	0	0	0	18	38	96	340	872
13	ARG115	14.93	0	0	0	0	0	0	0	0	0
14	ARG140	11.22	0	4	4	10	40	74	192	668	1908
15	ARG142	11.79	2	4	8	16	42	56	90	230	548
16	ARG147	9.10	92	182	496	1264	3384	9796	28046	80846	226790
17	ARG152	13.29	2	0	2	0	0	0	4	2	14
18	ARG153	12.00	0	0	0	2	2	12	32	96	310
19	ARG168	10.73	0	0	14	32	80	238	638	2008	5872
20	ARG169	12.54	0	0	0	0	2	0	6	14	54
21	ASP008	4.80	1207216	1508143	1028229	503705	200438	70224	24124	8124	2680
22	ASP021	4.18	1604964	814262	352546	138932	51122	17466	6050	2136	826
23	ASP038	4.54	1515987	965084	518369	254048	105450	38230	13172	4434	1642
24	ASP061	3.29	311268	132396	52270	19482	6738	2288	722	252	72
25	ASP064	4.62	1152229	1630624	876870	372588	137194	46960	15346	5122	1576
26	ASP073	4.99	813294	1473494	1390030	691062	282319	101742	35580	11678	3696
27	ASP096	4.31	1523611	904832	453098	193978	73962	27928	11344	4692	1812
28	ASP097	4.43	1565750	1257299	633382	260278	92820	30740	10296	3322	1102
29	ASP107	1.45	6876	2358	890	274	86	34	8	2	0
30	ASP108	2.07	25712	9452	3404	1400	442	156	34	22	2
31	ASP114	5.12	433154	1056159	1665802	810164	326122	124174	44922	15420	5048
32	ASP156	4.75	986935	1653361	1119676	493318	183126	63134	21738	7392	2546
33	ASP172	1.90	8018	3412	1538	656	244	94	28	12	4
34	CYS015	11.81	0	2	0	4	16	16	42	156	468
35	CYS018	12.07	0	2	2	2	2	8	28	88	282
36	CYS022	11.59	0	0	0	2	8	34	106	278	834
37	GLU007	5.00	733232	1387677	1501949	782490	329782	130234	54494	24066	9826
38	GLU017	5.30	445620	870076	1405852	1283262	585752	219458	75330	25962	9060
39	GLU046	4.94	528430	282706	216726	154856	109600	62484	27264	9690	3402
40	GLU094	5.19	384519	903696	1712407	1031340	431608	164446	60126	21579	7244
41	GLU104	3.42	649235	249132	87470	29006	9486	3190	1082	354	122
42	GLU120	4.81	909308	1630102	1122896	557450	267074	138782	79970	41420	18176
43	GLU128	2.88	201138	75580	26850	9896	4074	2162	1272	668	328
44	GLU135	4.25	1575144	782331	329837	127018	48358	18280	7544	3250	1592
45	GLU150	4.30	1629936	1072270	503488	198368	68900	22922	7642	2570	782
46	GLY001	5.29	343719	763334	1493171	1278115	571894	210808	72896	24882	8186
47	HIS014	7.54	4644	10964	25140	55532	129670	336078	849346	1762482	953834
48	HIS053	6.30	163624	217656	282837	557566	1240878	1400626	622448	230854	80382
49	HIS084	7.39	3618	7656	18664	52226	150686	425846	1064364	1632957	751248
50	HIS117	6.53	22072	59752	152516	374804	890453	1766880	953378	378898	131938
51	HIS122	7.29	36604	62834	97338	152512	282198	591766	1262877	1410771	632738
52	LYS002	9.80	388	542	736	1046	1572	2692	6752	18934	56178
53	LYS163	8.41	896	1694	3246	7292	18612	50054	137774	368724	913894
54	TYR174	4.61	817254	1712936	1022693	408946	142650	47274	14912	4898	1546

FIG. 4. The number of times each residue switched protonation states during Monte Carlo simulations of 10^8 iterations, at each of the pH values tabulated.

index	residue	$pK_{1/2}$	$pH = 4.5$		$pH = 7.1$	
			pK_{eff,α_*}	pK_{eff,α_*}	pK_{eff,α_*}	$pK_{int,\epsilon=3}$
01	R9	— ^a	12.09	12.45	11.30	
02	R31	—	11.90	12.90	11.30	
03	R36	—	13.78	14.04	11.30	
04	R47	11.57	10.88	11.33	11.30	
05	R58	11.33	10.45	10.70	11.30	
06	R59	—	14.17	14.66	11.30	
07	R76	11.80	11.02	11.50	11.30	
08	R79	—	9.20	9.48	11.30	
09	R89	—	14.29	14.33	11.30	
10	R91	—	11.82	11.88	11.30	
11	R95	11.89	10.85	11.54	11.30	
12	R99	12.00	11.25	11.47	11.30	
13	R115	—	14.69	14.93	11.30	
14	R140	11.55	10.96	11.22	11.30	
15	R142	—	10.82	11.79	11.30	
16	R147	9.45	8.80	9.10	11.30	
17	R152	—	13.06	13.29	11.30	
18	R153	—	11.46	12.00	11.30	
19	R168	11.73	10.51	10.73	11.30	
20	R169	—	12.39	12.54	11.30	
21	D8	4.42	4.29	4.80	5.41	
22	D21	3.88	3.90	4.18	5.41	
23	D38	3.91	3.89	4.54	5.41	
24	D61	2.73	3.11	3.29	5.41	
25	D64	4.39	4.38	4.62	5.41	
26	D73	4.72	4.79	4.99	5.41	
27	D96	3.82	3.94	4.31	5.41	
28	D97	4.09	4.23	4.43	5.41	
29	D107	—	1.31	1.45	5.41	
30	D108	1.60	1.85	2.07	5.41	
31	D114	4.91	4.89	5.12	5.41	
32	D156	4.57	4.67	4.75	5.41	
33	D172	—	1.33	1.90	5.41	
34	C15	—	11.32	11.81	12.00	
35	C18	—	11.27	12.07	12.00	
36	C22	—	11.33	11.59	12.00	
37	E7	4.79	4.85	5.00	5.80	
38	E17	5.17	5.14	5.30	5.80	
39	E46	3.14	3.26	4.94	5.80	
40	E94	5.03	4.97	5.19	5.80	
41	E104	3.25	3.37	3.42	5.80	
42	E120	4.59	4.59	4.81	5.80	
43	E128	2.44	2.84	2.88	5.80	
44	E135	3.86	3.88	4.25	5.80	
45	E150	4.01	4.10	4.30	5.80	
46	G1	5.19	5.13	5.29	4.88	
47	H14	7.54	6.91	7.54	7.05	
48	H53	6.28	6.14	6.30	6.04	
49	H84	7.40	7.29	7.39	6.91	
50	H117	6.53	6.20	6.53	6.37	
51	H122	7.27	6.13	7.29	6.32	
52	K2	9.83	8.78	9.80	7.98	
53	K163	8.50	8.05	8.41	7.98	
54	Y174	4.57	4.57	4.61	4.95	

^aValue not computed, see Supplemental Material text.

^b α_* denotes the most prominent configuration at the given pH .

FIG. 5. Residue-by-residue table of pK_{eff,α_*} at pH 4.5 and 7.1.

R91	E104	R89	E128	H84	R115	D107	R169	D108	R168	R58	Y174	R59	D172	R147	R79	D21	G1	C18	C22	D61	R36	D38	K2	E17	C15	H14
E104		4.2335	4.4197	2.5534	0.6990	0.1294	1.4631	0.1886	0.1312	0.4786	1.0931	0.7560	0.2210	0.1322	0.0447	0.0297	0.0346	0.0232	0.0336	0.0210	0.0152	0.0496	0.0071	0.0028	0.0034	0.0009
R89			4.4197	2.5534	0.6990	0.1294	1.4631	0.1886	0.1312	0.4786	1.0931	0.7560	0.2210	0.1322	0.0447	0.0297	0.0346	0.0232	0.0336	0.0210	0.0152	0.0496	0.0071	0.0028	0.0034	0.0009
E128				2.5534	0.6990	0.1294	1.4631	0.1886	0.1312	0.4786	1.0931	0.7560	0.2210	0.1322	0.0447	0.0297	0.0346	0.0232	0.0336	0.0210	0.0152	0.0496	0.0071	0.0028	0.0034	0.0009
H84					0.6990	0.1294	1.4631	0.1886	0.1312	0.4786	1.0931	0.7560	0.2210	0.1322	0.0447	0.0297	0.0346	0.0232	0.0336	0.0210	0.0152	0.0496	0.0071	0.0028	0.0034	0.0009
R115						0.1294	1.4631	0.1886	0.1312	0.4786	1.0931	0.7560	0.2210	0.1322	0.0447	0.0297	0.0346	0.0232	0.0336	0.0210	0.0152	0.0496	0.0071	0.0028	0.0034	0.0009
D107							1.4631	0.1886	0.1312	0.4786	1.0931	0.7560	0.2210	0.1322	0.0447	0.0297	0.0346	0.0232	0.0336	0.0210	0.0152	0.0496	0.0071	0.0028	0.0034	0.0009
R169								0.1886	0.1312	0.4786	1.0931	0.7560	0.2210	0.1322	0.0447	0.0297	0.0346	0.0232	0.0336	0.0210	0.0152	0.0496	0.0071	0.0028	0.0034	0.0009
D108									0.1312	0.4786	1.0931	0.7560	0.2210	0.1322	0.0447	0.0297	0.0346	0.0232	0.0336	0.0210	0.0152	0.0496	0.0071	0.0028	0.0034	0.0009
R168										0.4786	1.0931	0.7560	0.2210	0.1322	0.0447	0.0297	0.0346	0.0232	0.0336	0.0210	0.0152	0.0496	0.0071	0.0028	0.0034	0.0009
R58											1.0931	0.7560	0.2210	0.1322	0.0447	0.0297	0.0346	0.0232	0.0336	0.0210	0.0152	0.0496	0.0071	0.0028	0.0034	0.0009
Y174												0.7560	0.2210	0.1322	0.0447	0.0297	0.0346	0.0232	0.0336	0.0210	0.0152	0.0496	0.0071	0.0028	0.0034	0.0009
R59													0.2210	0.1322	0.0447	0.0297	0.0346	0.0232	0.0336	0.0210	0.0152	0.0496	0.0071	0.0028	0.0034	0.0009
D172														0.1322	0.0447	0.0297	0.0346	0.0232	0.0336	0.0210	0.0152	0.0496	0.0071	0.0028	0.0034	0.0009
R147															0.0447	0.0297	0.0346	0.0232	0.0336	0.0210	0.0152	0.0496	0.0071	0.0028	0.0034	0.0009
D39																0.0297	0.0346	0.0232	0.0336	0.0210	0.0152	0.0496	0.0071	0.0028	0.0034	0.0009
D21																	0.0346	0.0232	0.0336	0.0210	0.0152	0.0496	0.0071	0.0028	0.0034	0.0009
G1																		0.0232	0.0336	0.0210	0.0152	0.0496	0.0071	0.0028	0.0034	0.0009
C18																			0.0336	0.0210	0.0152	0.0496	0.0071	0.0028	0.0034	0.0009
C22																				0.0210	0.0152	0.0496	0.0071	0.0028	0.0034	0.0009
D61																					0.0152	0.0496	0.0071	0.0028	0.0034	0.0009
R36																						0.0496	0.0071	0.0028	0.0034	0.0009
D38																							0.0071	0.0028	0.0034	0.0009
K2																								0.0028	0.0034	0.0009
E17																									0.0034	0.0009
C15																										0.0009
H14																										0.0000

FIG. 6. Work-of-charging matrix modeled for Debye screening length 6\AA , first part. The order of residues is the same as in Fig. 2 of the Supplementary Material, and in Figs. 3(a), 16(a), and 16(b) of the text. Entries are in the dimensionless units of $e\phi_{ij}/k_B T$.

R91	E104	R89	E128	H84	R115	D107	R169	D108	R168	R58	Y174	R59	DI72	R147	R79	D21	G1	C18	C22	D61	R36	D38	K2	E17	C15	H14
E104		1.9171	0.7890	0.5631	0.2188	0.1753	0.1707	0.1160	0.0687	0.0367	0.0236	0.0142	0.0145	0.0273	0.0856	0.0623	0.0522	0.0232	0.0166	0.0146	0.0047	0.0033	0.0051	0.0049	0.0048	0.0025
R89				4.4382	0.9885	0.3587	0.4771	0.5534	0.3013	0.1530	0.0682	0.0495	0.0326	0.0267	0.0432	0.0535	0.0396	0.0256	0.0146	0.0107	0.0088	0.0055	0.0074	0.0064	0.0054	0.0029
E128								2.7241	0.3760	0.5172	0.5179	0.2105	0.0853	0.0663	0.0464	0.0406	0.0796	0.0696	0.0522	0.0596	0.0420	0.0216	0.0151	0.0121	0.0078	0.0112
H84											0.1860	0.1328	0.1972	0.3584	0.1540	0.0678	0.0525	0.0377	0.0462	0.0979	0.1407	0.1060	0.1355	0.0813	0.0420	0.0369
R115																										
D107																										
D108																										
R168																										
R58																										
Y174																										
R59																										
D172																										
R147																										
D21																										
C18																										
C22																										
D61																										
D38																										
K2																										
E17																										
C15																										
H14																										

FIG. 8. Work-of-charging matrix modeled for Debye screening length 12\AA , first part. The order of residues is the same as in Fig. 2 of the Supplementary Material, and in Figs. 3(a), 16(a), and 16(b) of the text. Entries are in the dimensionless units of $e\phi_{ij}/k_B T$.

R91	E104	R89	E128	H84	R115	D107	R169	D108	R168	R58	Y174	R59	DI72	R147	R79	D21	G1	C18	C22	D61	R36	D38	K2	E17	C15	H14		
		2.0334	0.8943	0.6646	0.2899	0.2338	0.2334	0.1649	0.1053	0.0617	0.0474	0.0372	0.0364	0.0566	0.1365	0.1070	0.0954	0.0522	0.0388	0.0367	0.0165	0.0133	0.0177	0.0176	0.0174	0.0110	0.0112	
E104			4.5662	1.0942	0.4375	0.5660	0.6518	0.3774	0.2110	0.1065	0.0870	0.0694	0.0581	0.0807	0.0905	0.0724	0.0753	0.0562	0.0347	0.0285	0.0261	0.0189	0.0236	0.0216	0.0191	0.0123	0.0098	
R89				4.7195	1.0685	0.4578	0.6111	0.6004	0.2731	0.1262	0.1075	0.0896	0.0786	0.1108	0.1113	0.0893	0.1030	0.0810	0.0463	0.0365	0.0324	0.0240	0.0314	0.0292	0.0257	0.0159	0.0120	
E128					2.8376	0.2076	0.2611	0.4252	0.2030	0.1062	0.0860	0.0758	0.0855	0.1514	0.2031	0.1619	0.2027	0.1361	0.0781	0.0637	0.0320	0.0268	0.0394	0.0399	0.0379	0.0217	0.0181	
R168						8.2385	0.3409	1.2741	0.8416	0.4056	0.2867	0.1557	0.1085	0.1159	0.0536	0.0421	0.0412	0.0425	0.0318	0.0205	0.0624	0.0378	0.0367	0.0277	0.0213	0.0172	0.0108	
R115							8.8416	1.8527	0.8527	0.4057	0.2867	0.1557	0.1085	0.1159	0.0536	0.0421	0.0412	0.0425	0.0318	0.0205	0.0624	0.0378	0.0367	0.0277	0.0213	0.0172	0.0108	
D107								1.3976	1.0300	0.4056	0.2865	0.1860	0.1271	0.1397	0.0493	0.0421	0.0449	0.0552	0.0337	0.0212	0.0660	0.0405	0.0413	0.0318	0.0242	0.0184	0.0108	
D108									4.6792	0.8944	0.3085	0.1860	0.1271	0.1397	0.0493	0.0421	0.0449	0.0552	0.0337	0.0212	0.0660	0.0405	0.0413	0.0318	0.0242	0.0184	0.0108	
R169										2.5084	1.7802	0.5280	0.4012	0.5205	0.0923	0.0835	0.0982	0.1309	0.0713	0.0394	0.1215	0.0739	0.0808	0.0621	0.0467	0.0331	0.0177	
D108											3.3450	0.4396	0.4342	0.4697	0.1092	0.1114	0.1012	0.1169	0.1463	0.0652	0.3089	0.1613	0.1374	0.0872	0.0647	0.0592	0.0318	
R168												1.0648	0.6139	0.7698	0.9938	0.0809	0.0913	0.1053	0.1601	0.1762	0.0702	0.4170	0.2116	0.1898	0.1169	0.0843	0.0732	0.0347
R58													1.0648	0.5095	0.0359	0.0372	0.0621	0.1660	0.0805	0.0401	0.3391	0.2029	0.2306	0.1598	0.1047	0.0758	0.0298	
R59														7.6493	0.0650	0.0711	0.1399	0.4784	0.1960	0.0822	0.5598	0.3465	0.5044	0.3309	0.2096	0.1315	0.0495	
D172															0.1457	0.1601	0.3417	1.1600	0.3909	0.1474	0.3291	0.2382	0.4028	0.3080	0.2222	0.1202	0.0547	
R79																6.5048	1.2252	0.2072	0.3302	0.3275	0.0338	0.0344	0.0498	0.0543	0.0676	0.0450	0.0642	
R147																	2.2090	0.2410	0.6407	0.3911	0.0514	0.0352	0.0616	0.0566	0.0848	0.0390	0.0922	
D21																		0.0741	1.0727	0.8634	0.6548	0.0711	0.4537	0.4079	0.4924	0.1850	0.1011	
G1																			1.2133	5.3169	0.3416	0.1845	0.2011	0.4537	0.4079	0.4924	0.1850	0.1011
C18																				5.3169	0.0845	0.1143	0.1590	0.1803	0.3133	0.2403	0.3752	
C22																					0.0845	0.1143	0.1590	0.1803	0.3133	0.2403	0.3752	
D61																					5.6158	1.0667	0.5201	0.3466	0.3429	0.0930		
R36																						1.6248	2.9218	1.4258	0.6480	0.7314	0.1562	
D38																												
K2																												
E17																												
C15																												
H14																												

FIG. 10. Work-of-charging matrix modeled for Debye screening length 20\AA , first part. The order of residues is the same as in Fig. 2 of the Supplementary Material, and in Figs. 3(a), 16(a), and 16(b) of the text. Entries are in the dimensionless units of $e\phi_{ij}/k_B T$.

